Muscle metaboreflex activation during hypercapnia modifies nonlinear heart rhythm dynamics, increasing the complexity of the sinus node autonomic regulation in humans

Stephane Delliaux, Masashi Ichinose, Kazuhito Watanabe, Naoto Fujii, Takeshi Nishiyasu

Muscle metaboreflex activation during hypercapnia modifies nonlinear heart rhythm dynamics, increasing the complexity of the sinus node autonomic regulation in humans

Stephane Delliaux,[1,2,4,5] Masashi Ichinose,[3,4] Kazuhito Watanabe,[4] Naoto Fujii,[4,5] and Takeshi Nishiyasu[4]

[1]*Aix Marseille Univ., INSERM, INRAE, C2VN, Marseille, France*
[2]*Assistance Publique – Hôpitaux de Marseille, APHM, Hôpital Nord, Pôle cardiovasculaire et thoracique, Laboratoire de Physiologie Respiratoire – Explorations à l'Exercice, Marseille, France*
[3]*School of Business and Administration, Meiji University, Tokyo, Japan*
[4]*Laboratory of Physiology – Circulation, Institute of Health and Sport Sciences, University of Tsukuba, Tsukuba, Japan*
[5]*Japan Society for the Promotion of Science, Tokyo, Japan*

Author contributions: S.D. conceptualized and designed the study, performed the experiments, processed the data, analyzed the results, wrote the manuscript, and led the research. M.I. gave advice on the study design, performed the experiments, analyzed the results, and discussed and critiqued the manuscript. K.W. gave advice on the experimental setup and performed the experiments. N.F. led the experimental setup, performed the experiments, analyzed the results and discussed the manuscript. T.N. gave advice on the study conception and design as well as the data processing and discussed and challenged the manuscript.

Running head: HRV during interaction of the muscle metaboreflex and hypercapnia

Corresponding author: Stephane Delliaux; stephane.delliaux@univ-amu.fr; Center for Cardiovascular and Nutrition Research, Faculté des Sciences Médicales et Paramédicales, Site Timone, 27 Bd Jean Moulin, 13385 Marseille Cedex 05, France

ABSTRACT [250 words]

Muscle metaboreflex activation during hypercapnia leads to enhanced pressive effects that are poorly understood while autonomic responses including baroreflex function are not documented. Thus, we assessed heart rate variability (HRV) that is partly due to autonomic influences on sinus node with linear tools (spectral analysis of instantaneous heart period), baroreflex set point and sensitivity with the heart period–arterial pressure transfer function and sequences methods, and system coupling through the complexity of RR interval dynamics with nonlinear tools (Poincaré plots and approximate entropy (ApEn)). We studied ten healthy young men at rest and then during muscle metaboreflex activation (MMA, postexercise muscle ischemia) and hypercapnia (HCA, PetCO2=+10 mmHg from baseline) separately and combined (MMA+HCA). The strongest pressive responses were observed during MMA+HCA, while baroreflex sensitivity was similarly lowered in the three experimental conditions. HRV was significantly different in MMA+HCA compared to MMA and HCA separately, with the lowest total power spectrum ($p<0.05$), including very low frequency ($p<0.05$), low-frequency ($p<0.05$), and high frequency (tendency) power spectra decreases, and the lowest Poincaré plot short term variability index (SD1): SD1=36.2 ms (MMA+HCA) vs. SD1=43.1 ms (MMA, $p<0.05$) and SD1=46.1 ms (HCA, $p<0.05$). Moreover, RR interval dynamics complexity was significantly increased only in the MMA+HCA condition (ApEn increased from 1.04±0.04, 1.07±0.02, and 1.05±0.03 to 1.10±0.03, 1.13±0.04, and 1.17±0.03 in MMA, HCA, and MMA+HCA conditions, respectively; $p<0.01$). These results suggest that in healthy young men, muscle metaboreflex activation during hypercapnia leads to interactions that reduce parasympathetic influence on the sinus node activity but complexify its dynamics.

KEYWORDS: muscle metaboreflex, hypercapnia, heart rate variability, heart rhythm dynamics, nonlinear

INTRODUCTION

Patients with chronic obstructive pulmonary disease, obstructive sleep apnea syndrome, and heart failure are known not only to develop muscle metaboreflex activation and hypercapnia but also to have increased arrhythmic morbidity and mortality rates [GAGNON P 2012[1], OLSON TP 2014[2], BRUCE RM 2016[3], GIANNONI A 2016[4], UENO-PARDI LM 2017[5]]. Nonetheless, the effects of muscle metaboreflex activation during hypercapnia on the heart are poorly documented.

Inspired by the pioneering works of Ponikowski et al. [PONIKOWSKI P 2001[6]] and Lykidis et al. [LYKIDIS CD 2009[7] and 2010[8]], we previously documented the cardiovascular response to forearm muscle metaboreflex activation during hypercapnia in healthy subjects [DELLIAUX S 2015[9]]. We reported partially additive pressor effects due to the attenuation of chronotropic and vasoconstrictive responses, the underlying mechanisms of which were not obvious.

Muscle metaboreflex activation in humans by postexercise muscle ischemia (PEMI) simultaneously increases parasympathetic and sympathetic influences on sinus activity [NISHIYASU T 1994[10], PIEPOLI M 1995[11], IELLAMO F 1999[12], FISHER JP 2010[13]]. However, this increase in the cardiac parasympathetic influence on sinus activity might reflect, at least in part, the buffering effects of the arterial baroreflex stimulated by the increased blood pressure [O'LEARY 1993[14], NISHIYASU 1994[10], IELLAMO F 1999[12], KIM JK 2005[15,16], WATANABE K 2010[17], INCOGNITO AV 2017[18]]. In addition, slight hypercapnia in dogs strongly increased both vagal and sympathetic discharges to the heart [KOLLAI M 1979[19]]. More recent pharmacological studies have confirmed the increasing effects of hypercapnia on cardiovagal activity [IKENOUE T 1981[20], SICA AL 2002[21]], and similar results have been found in humans [SASANO N 2002[22], BROWN SJ 2007[23]].

While muscle metaboreflex and hypercapnia generate signals that converge on common areas in the brain [SPYER KM 1994[24]] and stimulate cardiovascular function through the autonomic nervous system, the effects of muscle metaboreflex activation during hypercapnia on sinus node activity, its autonomic regulation and, therefore, heart rate dynamics in humans still need to be documented and characterized. To fill this gap, we tested the hypothesis that these combined cardiovascular stimuli increase parasympathetic modulation of sinus node activity.

To assess the neural component of sinus node activity control, we performed RR interval (RRI) and systolic blood pressure (SBP) time series analyses including heart rate

variability, mainly through spectral analysis. Because RRI time series are the result of a dynamically interacting complex system including muscle metaboreflex, hypercapnia, and arterial baroreflex inputs, the behavior of these time series might be nonlinear. To capture the nonlinear dynamics of heart rhythm, we also performed Poincaré plot analysis and approximate entropy (ApEn) estimation. ApEn is a family of statistics that quantify entropy and particularly the concept of changing complexity of the system [PINCUS SM 1991[25,26], 1994[27,28]]. ApEn has already been used and validated in the field of cardiac autonomic neuroscience [PINCUS SM 1992[29], FLEISHER LA 1993[30], AUBERT AE 2001[31], BOGAERT C 2001[32], BECKERS F 2001[33]].

Materials and methods

Subjects

Ten healthy young males were tested in this study. Their mean (± SEM) age, height and weight were 24±1 years, 1.73±0.01 m and 64±1 kg, respectively. All subjects had no history of smoking or taking any medication. Subjects were asked not to exercise for two days before their participation and not to drink alcohol, coffee or tea 12 hours before the experiment started. The study was approved by the Ethical Committee of the University of Tsukuba and was conducted in accordance with the Declaration of Helsinki. Each subject provided written consent. All experiments were conducted in the presence of a medical doctor.

Experimental procedures

Experimental procedures have been previously described [DELLIAUX S 2015[9]], and data were reanalyzed in an effort to better understand the mechanisms whereby the interaction between the metaboreflex and hypercapnia resulted in a hypo-additive heart rate response. Interventions consisted of measuring maximal voluntary contraction (MVC), stimulating the muscle metaboreflex, and performing a hyperventilation challenge. Subjects were asked to grip a hand dynamometer (digital dynamometer; TKK 5101; Takei, Niigata, Japan) and to perform three maximal voluntary contractions (MVCs) using their dominant arm. The highest of the three measurements was used in the experiment. Local circulatory occlusion was used to trap metabolites produced by contracting muscles, thereby evoking the muscle metaboreflex. Local circulatory occlusion with a suprasystolic pressure of 240 mmHg was achieved with a rapidly inflatable cuff placed on the upper

part of the dominant arm. The cuff pressure reached 240 mmHg in less than 1 s. The voluntary hyperventilation challenge consisted of calibrated hyperventilation. Breathing frequency (BF) was maintained at 20 breaths per min regulated by an electronic metronome, and a 1,500 ml tidal volume (Vt) was targeted (with visual feedback of the instantaneous Vt). N_2 and CO_2 supplies were adjusted to ensure normoxia and normocapnia or hypercapnia.

In a single experimental day, subjects performed three protocols in random order. Each protocol entailed a sequence of three periods: control, reflex activation and recovery. The control period was designed to provide 5 min of resting baseline data with normoxia, normocapnia and spontaneous breathing. Reflex activation was characterized by a 6-min experimental stimulus: 1) muscle metaboreflex activation (MMA), which consisted of a 1-min isometric handgrip exercise at 50% MVC (set from previous experiments and preliminary data) followed by a 5-min rest, all during normocapnia; 2) normoxic hypercapnia (HCA), which consisted of a 6-min rest with +10 mmHg end-tidal CO_2 partial pressure ($PetCO_2$) from baseline; and 3) muscle metaboreflex activation during hypercapnia (MMA+HCA). In all three protocols, dominant upper-arm ischemia induced by local circulatory occlusion and voluntary hyperventilation were maintained throughout the 6 min of Reflex Activation. Recovery consisted of a 5-min rest period (no exercise, no ischemia) under free air breathing conditions. The protocols were separated by rest periods of at least 30 min.

Measurements

Exclusive mouth breathing was ensured by having the subjects wear a nose clip. A mouthpiece was connected to a pneumotachograph and a T-shaped non-rebreathing Rudolph valve. N_2 and CO_2 supplies were controlled by manual flow meters connecting the inspiratory path to N_2 and CO_2 tanks. The expiratory path was opened to the room air. Inspiratory and expiratory gases were sampled at the mouthpiece level, and composition was analyzed by a mass spectrometer (Arco 2000; Arco System, Chiba, Japan). Analog signals for the respiratory variables, electrocardiogram (3-lead; Nihon Kohden, Tokyo, Japan), and arterial pressure waveform (finger photoplethysmography; Finometer; Finapres Medical System, Amsterdam, The Netherlands) were digitized at a sampling frequency of 1000 Hz (PowerLab 16/30 & LabChart Pro; ADinstruments Japan Inc., Nagoya, Japan) and fed into a personal computer.

We used Doppler ultrasound to evaluate stroke volume (SV). We measured ascending aortic blood velocity with a hand-held transducer probe (operating frequency: 2 MHz) connected to a Doppler ultrasound system (Echodoppler; HDI 3500; Atl/Philips Ultrasound, Bothwell, WA, USA). SV was calculated as the product of the aortic blood velocity (cm/s) and aortic cross-sectional area (cm^2), while aortic diameter was measured in a separate resting session.

Data analysis

Cardiorespiratory variables. We assessed the hemodynamic profile by measuring MAP (using digital photoplethysmography), heart rate (HR, using ECG), and SV (using echo Doppler), then calculated cardiac output as CO = SV × HR, from which we calculated total peripheral resistance as TPR = MAP / CO. We assessed the ventilatory profile through measured Vt, BF and Ve, and $PetCO_2$ and end-tidal O_2 partial pressure ($PetO_2$) obtained from respiratory flows (using pneumotachography) and respiratory gas analysis (using mass spectrometry), respectively. The ratio of inspiratory time to expiratory time (Ti/Te) has been used as an index of respiratory drive.

Baroreflex operating point and sensitivity. Baroreflex control of HR was determined from the relation and its spontaneous fluctuations (spontaneous arterial baroreflex) between HR and systolic pressure. The operating point was determined as the HR and SBP average values over 5 min for each period of the protocol, i.e., control, reflex activation (during the 5-min local circulatory occlusion), and recovery. Systolic pressure was used because HR correlates closely with systolic pressure but not with diastolic pressure [RUDAS L 1999[34]]. To ensure the reliability of spontaneous arterial baroreflex sensitivity (BRS) assessment, we applied two different methods, the sequences and the transfer function methods [BERTINIERI G 1985[35], PARATI G 1988[36], PINNA GD 2001[37]]. Concerning the sequences method, we first analyzed RRI and SBP beat-to-beat time series and identified sequences, i.e., all joint RRI and SBP increases or decreases involving at least 3 consecutive beats. The threshold change was set to 4 ms for RRI and 1 mmHg for SBP. For each sequence, linear regression between RRI and SBP was performed, and the regression coefficient was considered only if the correlation coefficient was ≥ 0.85. Mean value of the absolute values of the regression coefficients, i.e., the mean slope of rectified regression lines, was taken as a measure of the BRS. Concerning the transfer function method, we estimated BRS as the mean of RRI-SBP transfer function gains that had a squared coherence ≥ 0.85 in the frequency range of 0.05-0.15 Hz. The transfer function between RRI and SBP was calculated as

$$H(f) = S_{RRI.SBP}(f)/S_{RRI.RRI}(f)$$

where $S_{RRI.SBP}(f)$ is the cross-spectrum of RRI and SBP signals and $S_{RRI.RRI}(f)$ is the auto-spectrum of the RRI signal. Transfer function gain (magnitude) was obtained from the real part of the complex function $H(f)$, and the squared coherence function, which expresses the linear relationship between the input and output powers of the studied signals over the frequencies of interest, was calculated as

$$Coh(f) = |S_{RRI.SBP}(f)|^2/[S_{RRI.RRI}(f).S_{SBP.SBP}(f)]$$

where $S_{RRI.SBP}(f)$ is the cross-spectrum of RRI and SBP signals, and $S_{RRI.RRI}(f)$ and $S_{SBP.SBP}(f)$ are the auto-spectra of the RRI and SBP signals, respectively.

Autonomic influences on heart period. Heart rate variability (HRV) due to sympathovagal and more generally to autonomic effects on the sinoatrial node activity was assessed by spectral analysis according to guidelines [TASK FORCE 1996[38]]. We first visually checked all signals to remove and correct artifacts or too many frequent ectopic beats when necessary. Beat-to-beat RRI discrete time series were generated and then presented as a function of time. Cubic spline interpolation and resampling at 4 Hz converted the non-equidistantly sampled RR interval time series to 1200 points at equal time intervals. Then, we applied Welch's periodogram method for spectral density estimation. The RRI time series was divided into five equal ~66% overlapping segments of 512 points each. Linear detrending, Hanning windowing, and fast-Fourier transform were applied to each segment. The five generated spectra were averaged to provide spectrum estimates of the initial beat-to-beat RRI discrete time series. The spectral resolution was ~0.008 Hz. Total power (TP; 0–0.4 Hz), very low-frequency (VLF; <0.04 Hz) power, low-frequency (LF; 0.03–0.15 Hz) power and high-frequency (HF; 0.15–0.35 Hz) power were calculated by integrating spectral estimates over the frequency ranges of interest. LF and HF power were also expressed in normalized units (LFnu and HFnu, n.u.) and were calculated according to LF / (TP – VLF) x 100 and HF / (TP – VLF) x 100. HF in ms^2 and n.u. Finally, the ratio of LF [ms^2] to HF [ms^2] was calculated.

Poincaré plot. In some physiological and pathological states, concomitant sympathetic and parasympathetic activation can occur, leading to more complex autonomic modulation of sinus node activity. Acetylcholine and norepinephrine have a complex interaction at the level of the sinus node, resulting in a typical condition favoring the occurrence of complex HR dynamics (LEVY MN 1971[39], LEVY MN 1995[40]). The Poincaré plot, which is a diagram in which each RR interval of a tachogram is plotted as

a function of the previous RR interval (first recurrence map), seems to be a useful tool in such conditions [TULPPO MP 1998[41], BRENNAN M 2001[42], KOICHUBEKOV B 2017[43]]. An ellipse was fitted to the plot; the standard deviation (SD) of the plot data on the minor axis (SD1) described the instantaneous beat-to-beat variability, while the SD on the major axis (SD2) described the continuous long-term variability of the data. The ratio SD1/SD2 was also computed and characterizes the shape of Poincaré plots said to highlight nonlinear properties.

Regularity. We assessed the complexity of the nonlinear dynamical system that is the cardiovascular system by calculating the amount of regularity with approximate entropy (ApEn) [PINCUS M 1991[25,26], PINCUS M 1994[27,28]]. Entropy refers to system randomness, regularity and predictability and allows systems to be quantified by the rate of information loss or generation. ApEn more specifically measures the likelihood that runs of patterns that are close will remain close for subsequent incremental comparisons. In the present study, ApEn was calculated according to Pincus' formula [PINCUS M 1991[25]] with fixed input variables m = 2 and r = 15% (m being the length of the compared runs and r being a filter) [PINCUS SM 1994[27,28], GOLDBERGER AL 1994[44]]. Higher values of ApEn indicate a more complex structure in the time series. In this sense, ApEn rises with complexity and with interactions when applied to complex adaptive systems characterized by nonlinearly interacting components. ApEn was calculated as

$$\mathrm{ApEn}(m, r, N) = \Phi^m(r) - \Phi^{m+1}(r)$$

where $\Phi^m(r) = (N - m + 1)^{-1} . \sum_{i=1}^{N-m+1} \ln C_i^m(r)$, with N being the number of measured RRIs constituting the time series, m being a positive integer representing the length of the compared runs of data (i.e., the embedding dimension, where m=2), r is a positive real number specifying the filtering level (here, r=0.2. SD of RRI constituting the time series), and $C_i^m(r)$ is the relative number of vectors of length m for which $d(u_i, u_j) \leq \mathrm{r}\ \forall\ i \in (1,2,\dots,N-m+1)\ and\ \forall\ j$.

Statistics

Before any analysis we checked relevance of sample size for our purposes. To achieve a power of 80% (type II error) and a level of significance of 5% (two-sided type I error), for detecting an effect size of 1 (strong effect) on the approximate entropy (ApEn) between pairs as defined by Cohen's d formula, the study should have required a sample size of 11 (number of pairs). A posteriori calculation of Cohen's d showed that effect size effect was

very strong (equal to 4) in our experiment and that sample size = 10 was sufficient. Data are presented as the means ± SEMs. Statistical analyses were performed using 2-way repeated-measures ANOVA. The two factors for ANOVA were the period (control and reflex activation) and the experimental stimulus during reflex activation (HCA, MMA and MMA+HCA). When main effects were observed, post hoc procedures (Tukey's test after Bonferroni's correction) compared pairs of means. When appropriate, paired two-tailed t tests were also used. Values of $p<0.05$ were considered significant. Because of the poor quality of the echo Doppler signal during some periods of the voluntary hyperventilation challenge in 1 subject, some of his hemodynamic data were excluded.

RESULTS

Coactivation and cardiorespiratory macro-variables

The data during control and then during reflex activation periods in MMA, HCA and MMA+HCA conditions are summarized in table 1. Accordingly, there was no difference in any end-tidal, respiratory or hemodynamic variable at baseline across the three protocols, and the three experimental conditions led to HR, DBP, MBP, SBP, and CO increases ($p<0.001$). When compared to HCA, MMA pressive response led to higher DBP, MBP, and SBP but to similar chronotropic effects with comparable HR. In contrast, MMA+HCA led to the strongest cardiovascular response, including the highest HR, DBP, MBP, SBP, and CO increases, and interestingly led to the only SV significant increase from the control ($p=0.017$).

Coactivation and baroreflex function

Assessment of spontaneous arterial baroreflex function through determination of its operating point and sensitivity during control and then during MMA, HCA, and MMA+HCA is summarized in figure 1. In this figure, only the baroreflex sensitivities obtained from transfer function analysis are reported (oblique straight lines), and those from sequence analysis are strongly stackable to them and not significantly different ($p=0.937$). As shown, operating points as baroreflex sensitivities were similar across the three protocols at baseline. In contrast, reflex activation periods modified operating points accordingly to the experimental condition, i.e., on the one hand MMA and HCA and on the other hand MMA+HCA. MMA+HCA led to the strongest operating point change ($p<0.001$), including the highest SBP increase ($p<0.001$) and the deepest RRI decrease ($p<0.001$). In

addition, spontaneous arterial baroreflex sensitivity was lowered compared to the control ($p<0.001$) but similarly by MMA, HCA and MMA+HCA ($p=0.894$), from 19.71±2.99, 18.76±3.02, and 18.09±3.18 to approximately 13.33±1.97, 12.94±1.82, and 13.17±1.63 $ms.mmHg^{-1}$, respectively, i.e., approximately -30%.

Coactivation and HR dynamics

HRV and autonomic influences. RRIs were significantly and markedly lowered during MMA, HCA and MMA+HCA compared to the control ($p<0.001$), from 984±30ms, 1000±30ms and 968±29ms to 870±20ms, 833±15ms, and 789±15ms, respectively, as shown in figure 1. The evolution of the power spectra of the RRI time series according to the three protocols is summarized in table 2. On one hand, overall variability, as expressed by TP, which is equal to total variance, was significantly lowered only during the MMA+HCA condition ($p=0.0262$), reflecting mainly VLF and LF power decreases ($p=0.042$ and $p=0.0188$, respectively), HF power tending to decrease only ($p=0.068$). On the other hand, LFnu and HFnu were significantly lowered and increased, respectively, during MMA+HCA ($p=0.0189$) only. Therefore, the LF/HF ratio was significantly lowered only during the MMA+HCA condition ($p=0.0495$).

Nonlinear HR behavior. An illustrative example of a Poincaré plot from a representative subject is shown in figure 2, and statistics are reported in table 2. SD1, SD2, and SD1/SD2 were similar at baseline across the three protocols. Concerning SD1 and SD2, the MMA+HCA condition led to significant decreases ($p=0.0495$ and $p=0.02316$, respectively), while MMA and HCA tend to increase SD1 and had no significant effects on SD2. In contrast, SD1/SD2 was significantly ($p<0.001$) and similarly higher during MMA, HCA, and MMA+HCA.

Complexity. The evolution of ApEn during the protocol is summarized in Figure 3. Reflex activation periods increased ApEn ($p=0.000263$), but while MMA and HCA alone only tended to increase ApEn, the MMA+HCA condition was the only one to significantly increase ApEn (0.00633), and the sum of the ApEn increases induced by MMA on one side and HCA on the other side was lower ($p=0.000572$) than the ApEn increase induced by the MMA+HCA condition.

DISCUSSION

To better understand how muscle metaboreflex activation during hypercapnia leads to hypo-additive pressive and chronotropic effects [DELLIAUX S 2015[9]], we assessed the autonomic modulation of cardiovascular function from RRI and SBP time series analysis, including HRV analysis, spontaneous arterial baroreflex operating point and sensibility determination, and system coupling evaluation through RRI dynamics complexity in healthy young men. MMA+HCA led to the strongest pressive and chronotropic changes, while baroreflex sensitivity was similarly lowered in the three experimental conditions. The major findings of this study are the significant HR dynamics changes observed in the only MMA+HCA condition, including concomitant spectral powers (depending on parasympathetic system activity mainly) decrease and ApEn (complexity) increase. These findings suggest that in healthy young men, when the metaboreflex is activated under hypercapnic conditions, stimuli interactions lead to enhanced autonomic regulation of the cardiovascular function with a decreased parasympathetic influence on sinus node activity and a resetting of the spontaneous arterial baroreflex.

Complexity of HR dynamics

Our results strongly suggest otherwise demonstrate that muscle metaboreflex activation during hypercapnia leads to interacting cardiovascular responses. The increase in ApEn in the MMA+HCA condition indicates an interacting dynamical system. ApEn assesses and classifies complex systems, including both determinist chaotic and stochastic processes, according to their complexity [PINCUS SM[25,26,27,28]]. Large values of ApEn indicate the complex structure of a time series and the complex behavior of the system generating the time series. The more interacting the components of a system, the higher the complexity of the system [BARANGER M[45]]. The higher the complexity of the system is, the higher the ApEn [PINCUS SM[25,26,27,28]]. The present data show that complexity in HR dynamics increased during the MMA+HCA condition and that the sum of ApEn increases induced by MMA and HCA taken alone was lower ($p<0.001$) than the ApEn increase of MMA+HCA. These results support a synergistic interaction and therefore evoke rather a centrally-located interaction. This hypothesis seems to be corroborated by a recent study [SHAFER BM 2021[46]] performed on 13 young healthy males that reported a preserved muscle sympathetic nerve activity response to metaboreflex activation after acute hypercapnic hypoxia. Increased ApEn measures of RRI time series are rarely available in the literature. Nevertheless, it has been shown that under varying physiological conditions and in response to pharmacological denervation of arterial baroreceptors, the entropy of RRI time series could reflect parasympathetic modulation of

HR in conscious dogs [PALAZZOLO JA 1998[47]] and in humans [PENTTILA J 2003[48]]. What's more, high values of ApEn have been shown to decrease from childhood (highest values) to senescence (lowest values) [PIKKUJAMSA SM 1999[49]], and exercise has been associated with increased ApEn [TULPPO MP 2001[50]]. Accordingly, we can consider that during metaboreflex activation and hypercapnia, the sinus node undergoes the influence of various direct and indirect reflexes (metaboreflex, chemoreflex, baroreflex etc.) that "complexify" the behavior of heart rate on a beat-by-beat basis. Depending on the physiological scenario, parasympathetic and sympathetic components of the autonomic nervous system can work simultaneously and have cross-influence that, *in fine*, can be inhibitory or excitatory. This could be the case in our experiments and could explain why the complexity of the RR time series increases that cannot be precisely assessed via the linear indexes of HRV.

Autonomic influences

Indexes from RRI time series spectral analysis are known to be markers of the autonomic nervous system influences on the sinus node rhythmic activity. We found that TP and VLF, LF, and HF spectral powers decrease during the MMA+HCA condition. Besides, we found that LFnu and HFnu decrease and increase, respectively, during the MMA+HCA condition. According to first HRV guidelines [TASK FORCE 1996[38]], one could interpret these results as a sympathovagal balance change in aid of parasympathetic influence. On the contrary, at least three elements should alert us to a most judicious interpretation. First, a more recent and excellent review [REYES DEL PASO G 2013[51]] reminds us that scientific literature evidence pleads in favor of a mainly parasympathetic-determined HRV when assessed by spectral analysis indexes. Second, mathematical constructs of HRV normalized metrics can lead to confusing changes depending on whether LF and HF each other relatively vary as $LFnu = \frac{LF}{TP - VLF} \approx \frac{LF}{LF+HF}$ and $HFnu = \frac{HF}{TP - VLF} \approx \frac{HF}{LF+HF}$. Third, Poincaré plot short term variability index SD1 was lowered during MMA+HCA condition. SD1, that is the standard deviation of the plot data on the minor axis is mathematically equal to root mean square of successive differences of RRI duration described the instantaneous beat-to-beat variability that is neurally supported by the only vagal nerve [TULPPO MP 1996[52]]. This interpretation is more coherent with MMA+HCA effects on cardiovascular macro-variables as MMA+HCA led to significantly higher HR and MBP compared to MMA and HCA taken alone.

During PEMI, cardiac sympathetic [PIEPOLI M 1995[11], IELLAMO F 1999[12]] and parasympathetic [O'LEARY DS 1993[14], NISHIYASU T 1994[10]] influences have been shown to be simultaneously increased and to result from muscle metaboreflex and arterial baroreflex activations [FISHER JP 2010[13], WATANABE K 2010[17], DIPLA K 2013[53]] and their interactions [ICHINOSE M 2002[54], 2004[55], 2005[56]]. Usually, this leads to enhanced blood pressure, but PEMI-induced parasympathetic outflow to the sinus node overpowers the metaboreflex-induced cardiac sympathetic activation, limiting HR increase. Similarly, hypercapnia is known to be associated with increased HR and increased vagal and sympathetic modulation of sinus node activity [SASANO N 2002[22]], independent of any main direct effect on the baroreflex [COOPER VL 2005[57], SIMMONS GH 2007[58]]. In our study, we observed significantly lowered LF and SD2 in the only MMA+HCA condition, while BRS sensitivity was similar in the three experimental conditions. This suggests globally inhibitory effects on combined parasympathetic/sympathetic/baroreflex modulation [SHAFFER F 2017[59]] of sinus node activity. Because muscle metaboreflex and hypercapnia alone did not significantly decrease LF and SD2 powers, one can suppose that responses to MMA+HCA were triggered by their interactions. In our experiment, the complex system that led to RRI time series included at least three potentially interacting components: muscle metaboreflex, hypercapnia with direct humoral cardiovascular effects (hypercapnia *per se*) and indirect neurally supported cardiovascular effects (hypercapnia-evoked chemoreflex), and arterial baroreflex.

Baroreflex function

Even if the sum of the outputs of two systems taken separately is different from the output of two systems taken together, it cannot be assumed that they interact directly. In particular, our previous work could not exclude a limiting effect of the arterial baroreflex, such that the mechanisms of the observed hemodynamic responses were still unclear. Here, baroreflex resetting during reflex activation was different according to the experimental condition. In contrast, hemodynamic variable changes during MMA+HCA, which we previously attributed to reflex interactions [DELLIAUX S 2015[9]], seem not to be influenced by baroreflex function, as we found that BRS was similar in the three experimental conditions during the reflex activation periods, possibly as a result of resetting. Moreover, as the three experimental conditions led to the same magnitude of BRS decrease, it would be reasonable to think that a lower limit of baroreflex sensitivity was reached (a floor value, below which any measurements are out of range). The BRS values we observed are not unusual and as it has been previously reported that muscle

metaboreflex activation enhances BRS [SAMORA M[60]] and that hyperventilation lowers BRS (VAN DE BORNE P 2000[61]], it is more likely that a physiological condition common to the three experimental conditions could have driven BRS lowering. An obvious explanation could be the same respiratory pattern we set in the three experimental conditions.

Limitations and strengths of the study

A potential limitation of this study is that we did not directly assess sympathetic and parasympathetic tones. We used indirect indexes (spectral powers) from spectral analysis of RRI time series that are known to capture only linear properties of HR dynamics. Nevertheless, in stationary conditions, LF and HF, expressed in ms^2 as well as in normalized units, are largely thought to reflect sympathetic and parasympathetic modulatory effects on sinus node activity [TASK FORCE 1996[38]]. But as afore mentioned, a more recent review study [REYES DEL PASO G 2013[51]] compiling effects of manipulations affecting sympathetic and vagal activity on HRV, predictions of group differences in cardiac autonomic regulation from HRV, relationships between HRV and other cardiac parameters, and the theoretical and mathematical bases of the concept of autonomic balance evaluates the suitability of low LF heart rate variability as an index of sympathetic cardiac control and the LF/HF ratio as an index of autonomic balance. Authors concluded that available data challenge the interpretation of the LF and LF/HF ratio as indices of sympathetic cardiac control and autonomic balance, respectively, and suggest that the HRV power spectrum, including its LF component, is mainly determined by the parasympathetic system. Thus, LF and HF are said to be of limited interest in some physiological conditions, especially during interacting processes that, by definition, lead to nonlinear behavior [CASTIGLIONI P 2011[62], SILVA LE 2017[63]]. In relation to the complexity of the sinus node activity modulation system, predominantly nonlinear behavior must be assumed. Thus, the detailed description and classification of dynamic changes using time and frequency measures is often not sufficient. SD1 is known to be correlated with short-term HR variability [COPIE X 1996[64]] and HF [CONTRERAS P 2007[65], GUZIK P 2007[66]]. SD1 is also proposed as a marker of vagal activity [TOICHI M 1997[67]]. But Poincaré plot analysis and SD1 have been described as limited in their ability to capture nonlinear behavior, as the underlying metric is linear [BRENNAN M 2001[42], CICCONE AB 2017[68]], even if lag return maps are usually used to assess phase space in nonlinear phenomena. In contrast, ApEn is a tool that can assess nonlinear properties [PINCUS SM 1991[25,26], 1994[27,28]]. In general, high entropy is a characteristic of healthy

454 complex systems, in which regulatory mechanisms are working on their best performance
455 and, therefore, are capable of adapting to adverse conditions. Entropy has been described
456 to be correlated with vagal activity through pharmacological and physiological tests
457 [PENTILLÄ J 2003[48], BOLEA J 2014[69], SILVA LE 2017[70]] and at short scales would reflect
458 vagal modulation of HR [BARI V 2014[71], SILVA LE 2016[70], 2017[63]]. But observed ApEn
459 should not be considered as a mere expression of vagal activation since exercise, which is
460 known to notoriously lead to vagal withdrawal and sympathetic activation, is associated
461 with ApEn increase [TULPPO MP 2001[50]]. Evidence is still lacking to understand
462 precisely what are the changes in the sympathetic and parasympathetic modulations of
463 heart during MMA+HCA conditions.

464 Previous studies highlighted that HRV is dependent on the mean HR [PLATISA MM
465 2006[72,73], STAUSS HM 2014[74], MONFREDI O 2014[75], SACHA J 2014[76], GASIOR JS
466 2015[77]]. It is reasonable to think that the lower the heart period is, the more restricted its
467 range of variation will be. Nevertheless, autonomic influences on HRV cannot be
468 disregarded to the extent of considering HRV a surrogate of HR [DIAS DA SILVA VJ
469 2015[78], YANIV Y 2014[79]]. Here, we showed that even if MMA+HCA led to the highest HR
470 (shortest heart period), MMA+HCA also led to the increase in ApEn. Now, ApEn is
471 insensitive to HR variance. The ApEn method extracts the intrinsic dynamic properties of
472 the RR time series, and the algorithm disregards total variability through the tolerance
473 factor. This factor (r) was taken as a percentage of the time series standard deviation,
474 introducing a normalization procedure. Therefore, the results presented here can be
475 assumed to be related to cardiac autonomic modulation and not to the effect of different
476 mean HRs among subjects and conditions.

477 A second limitation of the study could be the necessary precaution or even caution to take
478 before generalizing these results. Three points needs to be addressed to consolidate
479 conclusions: even if our sample size was sufficient for a data re-analysis, it has not been
480 calculated on all variables of interest of the study that has not been designed accordingly;
481 female gender was not represented in our volunteer subjects, and all subjects were healthy
482 young men having daily physical activity. Further studies are needed to confirm and
483 generalize our first results.

484 *Perspective and Significance*

485 In conclusion, this study showed that, in healthy young men, the muscle metaboreflex
486 during hypercapnia modifies HRV dynamics. The interaction of physiological functions led

to highly nonlinear HRV behavior that needed to be assessed by appropriate tools. In this study, the variable of ApEn coupled with HRV spectral indexes and Poincaré plot SD1 inde highlighted that the muscle metaboreflex during hypercapnia modifies autonomic influences on the heart, particularly decreasing vagal modulation of the sinus node activity and complexifying its dynamics. In addition, our results strongly encourage the use of such nonlinear tools to study interactions between physiological functions.

493 **LEGENDS**

494 **FIGURE 1. Spontaneous arterial baroreflex set point and sensitivity during control and reflex**
495 **activation periods**

496 Set points (5-min average RRI (ms) as a function of 5-min average SBP (mmHg)) during control periods
497 (circles) and reflex activation periods (triangles) are plotted according to the experimental condition,
498 i.e., MMA (white), HCA (light gray), and MMA+HCA (dark grey). Set-points are shown as the means
499 (markers) ± SEMs (error bars). The BRS values of the control and reflex activation periods are
500 represented by continuous and dashed lines, respectively. ***, significant difference vs. control at
501 $p<0.001$; ### significant difference vs. MMA at $p<0.001$; £££, ££, significant difference vs. HCA at
502 $p<0.001$ and $p<0.01$, respectively. There was no difference in BRS across the three reflex activation
503 periods: NS, nonsignificant.

504

505 **FIGURE 2. Representative subject data: tachograms, power spectra, and Poincaré plots under the**
506 **MMA, HCA, and MMA+HCA experimental conditions**

507 Tachograms, power spectra, and Poincaré plots of a representative subject are reported in the upper,
508 middle, and lower panels, respectively, with the MMA, HCA, and MMA+HCA experimental conditions
509 presented in the left, middle, and right panels, respectively. Tachograms represent the RR interval (RRI,
510 ms) as a function of time (min) of the running protocol and the corresponding phases that consisted
511 of rest (5 min); muscle contraction, if any (1 min, MMA, and MMA+HCA); and venous occlusion (5 min)
512 leading to PEMI when contraction occurred. Power spectra express the power density (ms^2) of the RRI
513 as a function of frequency (Hz) according to protocol periods, i.e., rest (dashed gray line) and reflex
514 activation (continuous black line). Poincaré plots (scatter plots) represent the n^{th} RRI (ms) as a function
515 of the $n\text{-}1^{th}$ RRI (previous beat, ms) of the RRI time series corresponding to rest (gray markers and line)

and reflex activation (dark markers and line) periods. Lines are shown to illustrate the complexity trajectory of RRI pairs.

FIGURE 3. Approximate entropy of the RR interval (RRI) during control and reflex activation periods

Approximate entropy (ApEn, unitless) values are box plotted (median, 25-75th percentiles, and 1-99th percentiles) as a function of phase experiments (control and reflex activation) according to experimental condition: MMA (white), HCA (light gray), and MMA+HCA (dark gray). *** $p<0.001$ for reflex activation vs. control when MMA, HCA, and MMA+HCA data are aggregated (phase effect with ANOVA); ** $p<0.01$ for reflex activation vs. control in the MMA+HCA experimental condition (condition effect with ANOVA); $^{\#}$ $p<0.05$ for MMA+HCA vs. MMA; ^{T} $0.05<p<0.1$ for MMA+HCA vs. HCA. ApEn is significantly enhanced in the MMA+HCA condition.

TABLE 1. Cardiorespiratory macro-variables during control (Baseline) and reflex activation (Reflex) periods

Values are means ± SEMs. Control, resting period with free breathing and no stimulus; reflex activation, period defined by the experimental conditions (voluntary hyperventilation and local circulatory occlusion in the dominant arm plus hypercapnia or muscle metaboreflex activation or hypercapnia plus muscle metaboreflex activation). $PetCO_2$, end-tidal partial pressure of CO_2; $PetO_2$, end-tidal partial pressure of O_2; Ve, minute-ventilation calculated from the raw data and then rounded to the nearest significant digit; BF, breathing frequency; Vt, tidal volume; Ti/Te, inspiratory time/expiratory time; HR, heart rate; SBP, systolic blood pressure; MBP, mean blood pressure; DBP, diastolic blood pressure; CO, cardiac output; SV, stroke volume. *, **, ***, significant difference vs. control at $p<0.05$, $p<0.01$, and $p<0.001$, respectively; $^{\#}$, $^{\#\#}$, $^{\#\#\#}$ significant difference vs. MMA at $p<0.05$, $p<0.01$, and $p<0.001$, respectively; $^{£}$, $^{££}$, $^{£££}$ significant difference vs. HCA at $p<0.05$, $p<0.01$, and $p<0.001$, respectively.

TABLE 2. HRV during control (Baseline) and reflex activation (Reflex) periods

Values are means (rounded to the nearest significant digit) ± SEMs of spectral analysis and Poincaré plot indexes calculated from the 5-min RRI time series. Control, resting period with free breathing and no stimulus; reflex activation, period defined by the experimental conditions (voluntary hyperventilation and local circulatory occlusion in the dominant arm plus hypercapnia or muscle metaboreflex activation or hypercapnia plus muscle metaboreflex activation). HCA, hypercapnia; MMA, muscle metaboreflex activation; MMA+HCA, muscle metaboreflex activation during hypercapnia; TP, total power; VLF, very low-frequency power; LF, low-frequency power; HF, high-frequency power; LFnu, low-frequency power in normalized units; HFnu, high-frequency power in normalized units; LF/HF, low-frequency power to high-frequency power ratio; SD1, standard deviation of points along the minor axis (perpendicular to the line of identity) of a fitted ellipse; SD2, standard deviation of points along the major axis (along the line of identity) of a fitted ellipse; SD1/SD2, SD1 to SD2 ratio. ^{T}, *, **, ***, significant difference vs. control at $0.05<p<0.1$, $p<0.05$, $p<0.01$, and $p<0.001$, respectively; $^{\#}$, $^{\#\#}$, significant difference vs. MMA at $p<0.05$ and $p<0.01$, respectively; $^{£}$ significant difference vs. HCA at $p<0.05$.

TABLE 1. Cardiorespiratory macro-variables during control (Baseline) and reflex activation (Reflex) periods

	MMA		HCA		MMA+HCA	
	Baseline	**Reflex**	**Baseline**	**Reflex**	**Baseline**	**Reflex**
$PetCO_2$, mmHg	46.1±0.7	46.7±0.8	45.9±0.6	56.8±0.5$^{***,\#\#\#}$	46.0±0.7	56.8±0.7$^{***,\#\#\#}$
$PetO_2$, mmHg	100±1	102±1	100±1	102±1	100±1	101±1
Ve, $L.min^{-1}$	8.5±0.4	29.5±0.5***	8.1±0.4	31.4±0.5$^{***,\#\#}$	8.2±0.3	31.9±0.4$^{***,\#\#}$
BF, min^{-1}	13±1	20±0***	12±1	20±0***	12±1	20±0***
Vt, L	0.7±0.0	1.5±0.0***	0.7±0.0	1.6±0.0$^{***,\#}$	0.7±0.1	1.6±0.0$^{***,\#}$
Ti/Te, no units	68±4	97±3***	62±3	90±2$^{***,\#\#}$	71±5	85±3$^{***,\#\#}$
HR, min^{-1}	61±3	69±3**	60±3	72±4***	62±3	76±4$^{***,\#\#\#,££}$
SBP, mmHg	119±3	146±3***	117±4	137±4$^{***,\#\#\#}$	123±6	163±6$^{***,\#\#\#,£££}$
MBP, mmHg	79±2	101±2***	80±3	91±3$^{**,\#}$	82±3	110±3$^{***,\#\#,£££}$
DBP, mmHg	60±2	78±2**	61±3	69±3$^{*,\#}$	62±3	82±3$^{***,\#,£}$
CO, $L.min^{-1}$	5.21±0.42	6.48±0.24**	5.02±0.24	6.44±0.47**	5.12±0.27	7.44±0.45$^{***,\#\#,££}$
SV, mL	86±3	94±3	84±3	89±3	84±4	98±4$^{*,\#,£}$

561 **FIGURE 1. Spontaneous arterial baroreflex set point and sensitivity during control and reflex**
562 **activation periods**

563

564

565

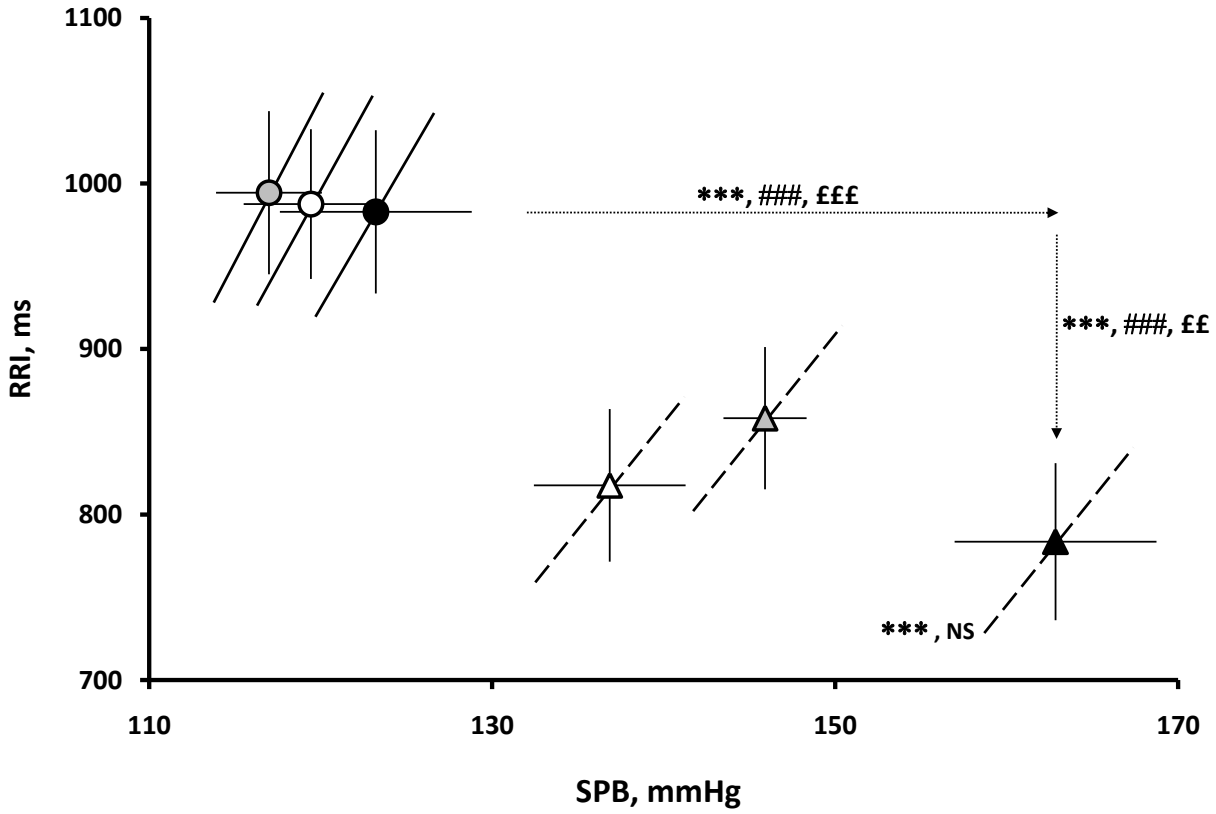

566 **TABLE 2. HRV during control (Baseline) and reflex activation (Reflex) periods**

	MMA		HCA		MMA+HCA	
	Baseline	**Reflex**	**Baseline**	**Reflex**	**Baseline**	**Reflex**
Spectral analysis						
TP, ms^2	4530±1277	2185±539	4256±1152	2311±803	4441±948	1485±297*
VLF, ms^2	898±379	378±63	1205±396	507±100	1137±343	326±70*
LF, ms^2	1891±1010	452±108	1361±619	316±74	1386±398	267±87$^{*,\#}$
HF, ms^2	1741±591	1355±501	1689±504	1489±671	1918±691	892±217
LFnu, n.u.	42.6±7.4	33.3±6	39.1±8.2	27.7±4.8	46.4±9.5	25.0±5.3$^{*,\#,£}$
HFnu, n.u.	57.4±7.4	66.7±6	60.9±8.2	72.2±4.8	53.6±9.5	75.0±5.3$^{*,\#,£}$
LF/HF	1.09±0.5	0.33±0.1^{T}	0.80±0.4	0.21±0.1	0.72±0.4	0.29±0.0*
Poincaré plot						
SD1, ms	38.3±7.1	43.1±7.0	35.5±7.6	46.1±9.4	39.8±8.2	36.2±6*
SD2, ms	70.9±9.9	52.6±5.0	66.8±12.3	53.0±6.4	74.6±11.5	47.6±3.9*
SD1/SD2	0.54±0.06	0.8±0.008***	0.53±0.04	0.87±0.09**	0.53±0.07	0.76±0.08**

567

568

FIGURE 2. Representative subject data: tachograms, power spectra, and Poincaré plots under the MMA, HCA, and MMA+HCA experimental conditions

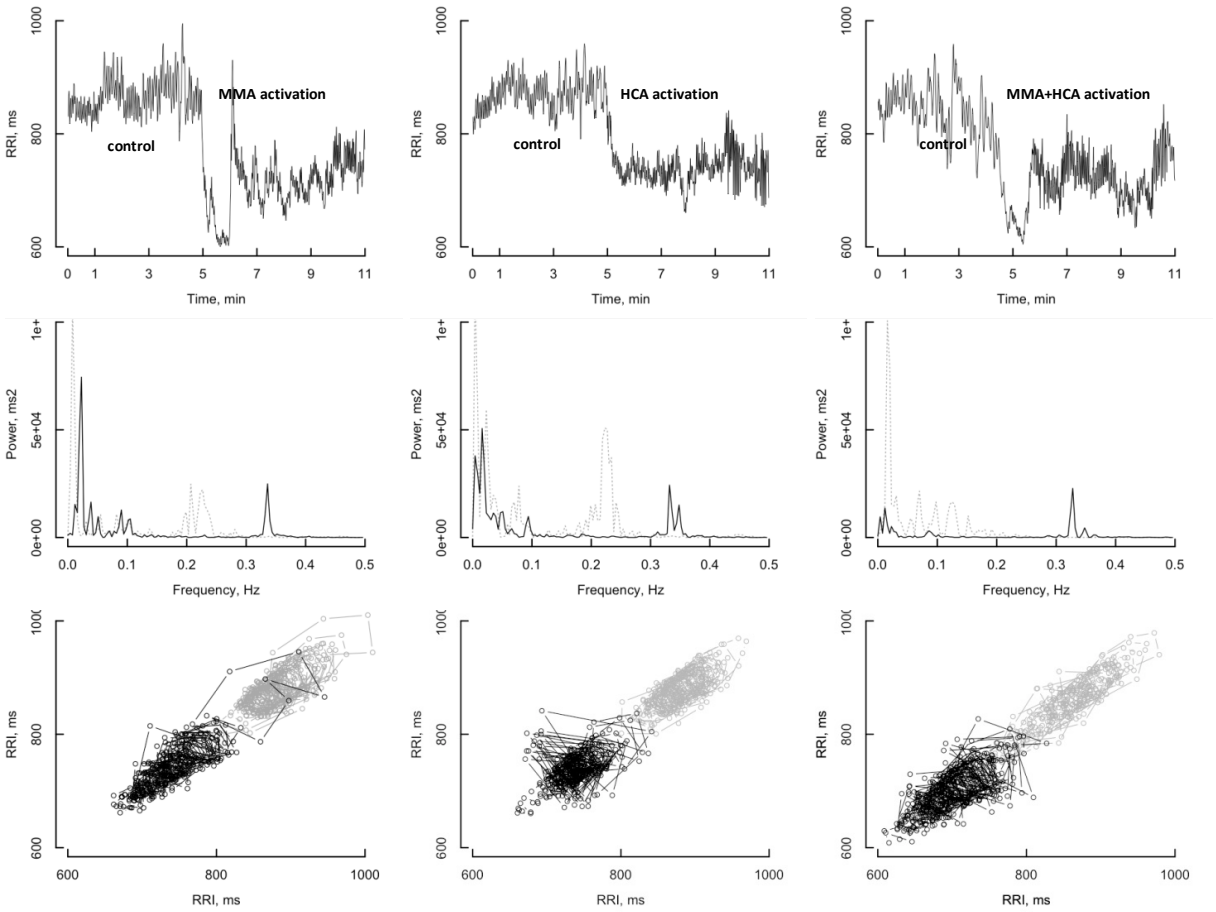

574 **FIGURE 3. Approximate entropy of the RR interval (RRI) during control and reflex activation periods**

575

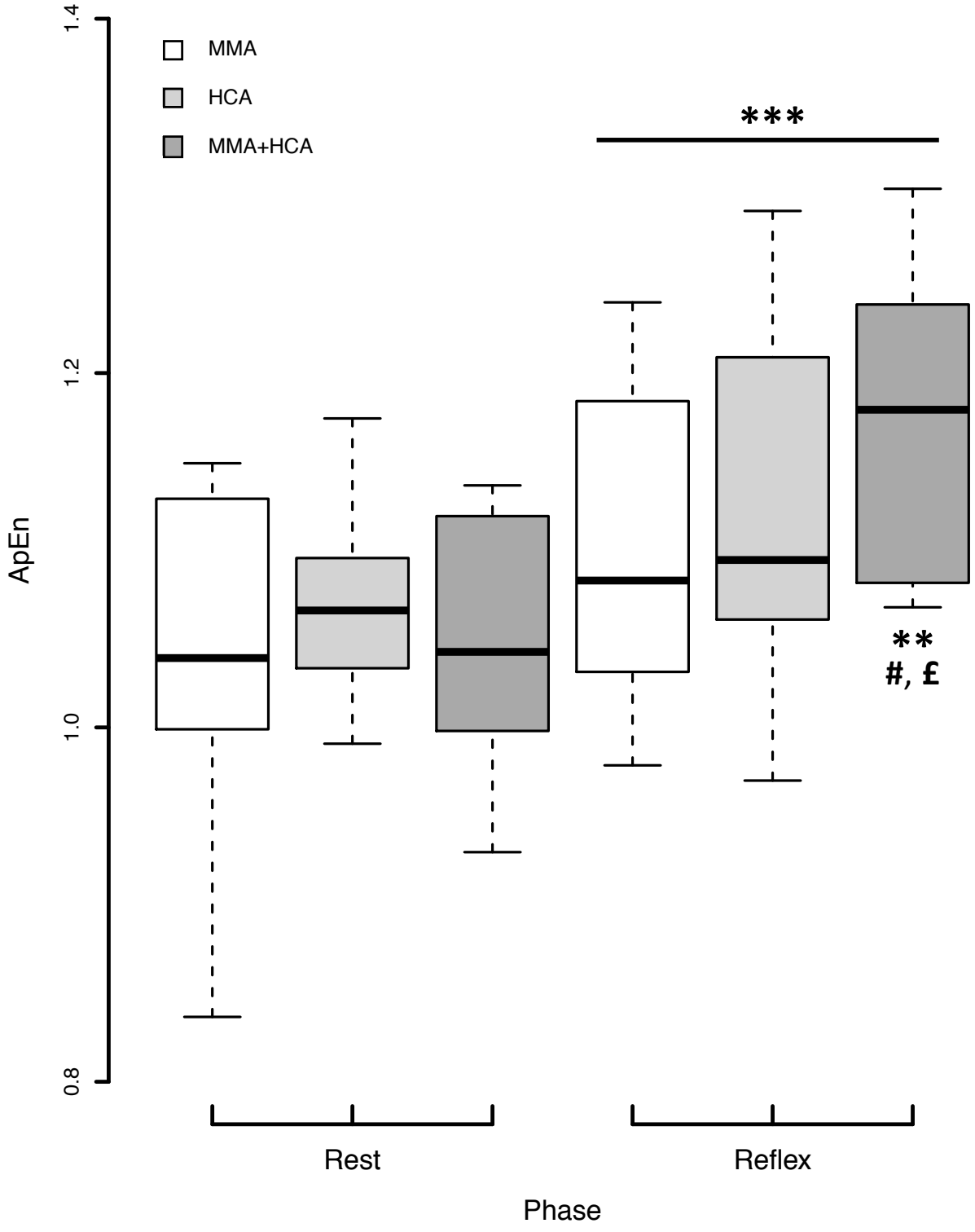

576

577

578

DECLARATIONS

Ethical Approval

The study was approved by the Ethical Committee of the University of Tsukuba and was conducted in accordance with the Declaration of Helsinki. Each subject provided written consent.

Competing interests

Authors declare to have no competing interests.

Authors' contributions

S.D. conceptualized and designed the study, performed the experiments, processed the data, analyzed the results, wrote the manuscript, and led the research. M.I. gave advice on the study design, performed the experiments, analyzed the results, and discussed and critiqued the manuscript. K.W. gave advice on the experimental setup and performed the experiments. N.F. led the experimental setup, performed the experiments, analyzed the results and discussed the manuscript. T.N. gave advice on the study conception and design as well as the data processing and discussed and challenged the manuscript.

Funding

S.D. has been granted by the Japan Society for the Promotion of Science (JSPS) to lead this research with the short-term postdoctoral JSPS fellowship.

The project leading to this publication has received funding via Läennec institute from the Excellence Initiative of Aix-Marseille Université - A*Midex, a French “Investissements d’Avenir programme” AMX-21-IET-017.

Availability of data and materials

Data are available on reasonable request to the corresponding author.

603 REFERENCES

[1] Gagnon P, Bussières JS, Ribeiro F, Gagnon SL, Saey D, Gagné N, Provencher S & Maltais F (2012). Influences of spinal anesthesia on exercise tolerance in patients with chronic obstructive pulmonary disease. Am J Respir Crit Care Med 186, 606–615.

[2] Olson TP, Joyner MJ, Eisenach JH, Curry TB & Johnson BD (2014). Influence of locomotor muscle afferent inhibition on the ventilatory response to exercise in heart failure. Exp Physiol 99, 414–426.

[3] Bruce RM, Turner A, White MJ. Ventilatory responses to muscle metaboreflex activation in chronic obstructive pulmonary disease. J Physiol. 2016 Oct 15;594(20):6025-6035.

[4] Giannoni A, Raglianti V, Mirizzi G, Taddei C, Del Franco A, Iudice G, Bramanti F, Aimo A, Pasanisi E, Emdin M, Passino C. Influence of central apneas and chemoreflex activation on pulmonary artery pressure in chronic heart failure. Int J Cardiol. 2016 Jan 1;202:200-6.

[5] Ueno-Pardi LM, Guerra RS, Goya TT, Silva RF, Gara EM, Lima MF, Nobre TS, Alves MJNN, Trombetta IC, Lorenzi-Filho G. Muscle Metaboreflex Control of Sympathetic Activity in Obstructive Sleep Apnea. Med Sci Sports Exerc. 2017 Jul;49(7):1424-1431.

[6] Ponikowski P, Francis DP, Piepoli MF, Davies LC, Chua TP, Davos CH, Florea V, Banasiak W, Poole-Wilson PA, Coats AJ, Anker SD. Enhanced ventilatory response to exercise in patients with chronic heart failure and preserved exercise tolerance: marker of abnormal cardio-respiratory reflex control and predictor of poor prognosis. Circulation 103: 967–972, 2001.

[7] Lykidis CK, Kumar P, Balanos GM. The respiratory responses to the combined activation of the muscle metaboreflex and the ventilatory chemoreflex. Adv Exp Med Biol 648: 281–287, 2009.

[8] Lykidis CK, Kumar P, Vianna LC, White MJ, Balanos GM. A respiratory response to the activation of the muscle metaboreflex during concurrent hypercapnia in man. Exp Physiol 95: 194–201, 2010.

[9] Delliaux S, Ichinose M, Watanabe K, Fujii N, Nishiyasu T. Cardiovascular responses to forearm muscle metaboreflex activation during hypercapnia in Humans. Am J Physiol Regul Integr Comp Physiol. 2015 Jul 1;309(1):R43-50.

[10] Nishiyasu T, Tan N, Morimoto K, Nishiyasu M, Yamaguchi Y, Murakami N. Enhancement of parasympathetic cardiac activity during activation of muscle metaboreflex in humans. J Appl Physiol (1985). 1994 Dec;77(6):2778-83.

[11] Piepoli M, Clark AL, Coats AJ. Muscle metaboreceptors in hemodynamic, autonomic, and ventilatory responses to exercise in men. Am J Physiol. 1995 Oct;269(4 Pt 2):H1428-36.

[12] Iellamo F, Pizzinelli P, Massaro M, Raimondi G, Peruzzi G, Legramante JM. Muscle metaboreflex contribution to sinus node regulation during static exercise: insights from spectral analysis of heart rate variability. Circulation. 1999 Jul 6;100(1):27-32.

[13] Fisher JP, Seifert T, Hartwich D, Young CN, Secher NH, Fadel PJ. Autonomic control of heart rate by metabolically sensitive skeletal muscle afferents in humans. J Physiol. 2010 Apr 1;588(Pt 7):1117-27.

[14] O'Leary DS. Autonomic mechanisms of muscle metaboreflex control of heart rate. J Appl Physiol (1985). 1993 Apr;74(4):1748-54.

[15] Kim JK, Sala-Mercado JA, Rodriguez J, Scislo TJ, O'Leary DS. Arterial baroreflex alters strength and mechanisms of muscle metaboreflex during dynamic exercise. Am J Physiol Heart Circ Physiol. 2005 Mar;288(3):H1374-80.

[16] Kim JK, Sala-Mercado JA, Hammond RL, Rodriguez J, Scislo TJ, O'Leary DS. Attenuated arterial baroreflex buffering of muscle metaboreflex in heart failure. Am J Physiol Heart Circ Physiol. 2005 Dec;289(6):H2416-23.
[17] Watanabe K, Ichinose M, Fujii N, Matsumoto M, Nishiyasu T. Individual differences in the heart rate response to activation of the muscle metaboreflex in humans. Am J Physiol Heart Circ Physiol. 2010 Nov;299(5):H1708-14.
[18] Incognito AV, Doherty CJ, Lee JB, Burns MJ, Millar PJ. Inter-individual variability in muscle sympathetic responses to static handgrip in young men: Evidence for sympathetic responder types? Am J Physiol Regul Integr Comp Physiol. 2017 Oct 25:ajpregu.00266.2017.
[19] Kollai M, Koizumi K. Reciprocal and non-reciprocal action of the vagal and sympathetic nerves innervating the heart. J Auton Nerv Syst. 1979 Oct;1(1):33-52.
[20] Ikenoue T, Martin CB Jr, Murata Y, Ettinger BB, Lu PS. Effect of acute hypoxemia and respiratory acidosis on the fetal heart rate in monkeys. Am J Obstet Gynecol. 1981 Dec 1;141(7):797-806.
[21] Sica AL, Ruggiero DA, Zhao N, Gootman PM. Developmental changes in heart rate variability during exposure to prolonged hypercapnia in piglets. Auton Neurosci. 2002 Sep 30;100(1-2):41-9.
[22] Sasano N, Vesely AE, Hayano J, Sasano H, Somogyi R, Preiss D, Miyasaka K, Katsuya H, Iscoe S, Fisher JA. Direct effect of Pa(CO2) on respiratory sinus arrhythmia in conscious humans. Am J Physiol Heart Circ Physiol. 2002 Mar;282(3):H973-6.
[23] Brown SJ, Mundel T, Brown JA. Cardiac vagal control and respiratory sinus arrhythmia during hypercapnia in humans. J Physiol Sci. 2007 Dec;57(6):337-42.
[24] Spyer KM. Annual review prize lecture. Central nervous mechanisms contributing to cardiovascular control. J Physiol. 1994 Jan 1;474(1):1-19.
[25] Pincus SM. Approximate entropy as a measure of system complexity. Proc Natl Acad Sci U S A. 1991 Mar 15;88(6):2297-301.
[26] Pincus SM, Gladstone IM, Ehrenkranz RA. A regularity statistic for medical data analysis. J Clin Monit. 1991 Oct;7(4):335-45.
[27] Pincus SM, Goldberger AL. Physiological time-series analysis: what does regularity quantify? Am J Physiol. 1994 Apr;266(4 Pt 2):H1643-56.
[28] Pincus SM. Greater signal regularity may indicate increased system isolation. Math Biosci. 1994 Aug;122(2):161-81.
[29] Pincus SM, Viscarello RR. Approximate entropy: a regularity measure for fetal heart rate analysis. Obstet Gynecol. 1992 Feb;79(2):249-55.
[30] Fleisher LA, Pincus SM, Rosenbaum SH. Approximate entropy of heart rate as a correlate of postoperative ventricular dysfunction. Anesthesiology. 1993 Apr;78(4):683-92.
[31] Aubert AE, Beckers F, Ramaekers D. Short-term heart rate variability in young athletes. J Cardiol. 2001;37 Suppl 1:85-8.
[32] Bogaert C, Beckers F, Ramaekers D, Aubert AE. Analysis of heart rate variability with correlation dimension method in a normal population and in heart transplant patients. Auton Neurosci. 2001 Jul 20;90(1-2):142-7.
[33] Beckers F, Ramaekers D, Aubert AE. Approximate entropy of heart rate variability: Validation of methods and application in heart failure. Cardiovasc. Eng. 2001; 1: 177– 82.
[34] Rudas L, Crossman AA, Morillo CA, Halliwill JR, Tahvanainen KU, Kuusela TA, Eckberg DL. Human sympathetic and vagal baroreflex responses to sequential nitroprusside and phenylephrine. Am J Physiol. 1999 May;276(5 Pt 2):H1691-8.

[35] Bertinieri G, Di Rienzo M, Cavallazzi A, Ferrari AU, Pedotti A, Mancia G (1985) A new approach to analysis of the arterial baroreflex. J Hypertens Suppl 3:S79–S81
[36] Parati G, Di Rienzo M, Bertinieri G, Pomidossi G, Casadei R, Groppelli A, Pedotti A, Zanchetti A, Mancia G. Evaluation of the baroreceptor-heart rate reflex by 24-hour intra-arterial blood pressure monitoring in humans. Hypertension. 1988 Aug;12(2):214-22.
[37] Pinna GD, Maestri R (2001) Reliability of transfer function estimates in cardiovascular variability analysis. Med Biol Eng Comput 39:338–347
[38] Heart rate variability: standards of measurement, physiological interpretation and clinical use. Task Force of the European Society of Cardiology and the North American Society of Pacing and Electrophysiology. Circulation. 1996 Mar 1;93(5):1043-65.
[39] Levy, M. N. Sympathetic-parasympathetic interactions in the heart. Circ. Res. 29: 437–445, 1971.
[40] Levy M.N. Time dependency of the autonomic interactions that regulate heart rate and rhythm. In: Cardiac Electrophysiology. From Cell to Bedside, edited by D. Zipes and J. Jalife. Philadelphia, PA: Saunders, 1995, p. 454–459.
[41] Tulppo MP, Mäkikallio TH, Seppänen T, Airaksinen JK, Huikuri HV. Heart rate dynamics during accentuated sympathovagal interaction. Am J Physiol. 1998 Mar;274(3 Pt 2):H810-6.
[42] Brennan M, Palaniswami M, Kamen P. Do existing measures of Poincaré plot geometry reflect nonlinear features of heart rate variability? IEEE Trans Biomed Eng. 2001 Nov;48(11):1342-7.
[43] Koichubekov B, Riklefs V , Sorokina M , Korshukov I, Turgunova L, Laryushina Y, Bakirova R, Muldaeva G, Bekov E and Kultenova M. Informative nature and nonlinearity of lagged Poincaré plots indices in analysis of heart rate variability. Entropy 2017, 19, 523; doi:10.3390/e19100523.
[44] Goldberger AL, Mietus JE, Rigney DR, Wood ML, Fortney SM. Effects of head-down bed rest on complex heart rate variability: response to LBNP testing. J Appl Physiol (1985). 1994 Dec;77(6):2863-9.
[45] Baranger M. Chaos, Complexity, and Entropy. A physics talk for non-physicists. Center for Theoretical Physics, Laboratory for Nuclear Science and Department of Physics Massachusetts Institute of Technology, Cambridge, MA 02139, USA and New England Complex Systems Institute, Cambridge, MA 02138, USA MIT-CTP-3112
[46] Shafer BM, Incognito AV, Vermeulen TD, Nardone M, Teixeira AL, Benbaruj J, Millar PJ, Foster GE. Muscle Metaboreflex Control of Sympathetic Activity Is Preserved after Acute Intermittent Hypercapnic Hypoxia. Med Sci Sports Exerc. 2021 Nov 1;53(11):2233-2244.
[47] Palazzolo JA, Estafanous FG, Murray PA. Entropy measures of heart rate variation in conscious dogs. Am J Physiol. 1998 Apr;274(4 Pt 2):H1099-105.
[48] Penttilä J, Helminen A, Jartti T, Kuusela T, Huikuri HV, Tulppo MP, Scheinin H. Effect of cardiac vagal outflow on complexity and fractal correlation properties of heart rate dynamics. Auton Autacoid Pharmacol. 2003 Jun;23(3):173-9.
[49] Pikkujämsä SM, Mäkikallio TH, Sourander LB, Räihä IJ, Puukka P, Skyttä J, Peng CK, Goldberger AL, Huikuri HV. Cardiac interbeat interval dynamics from childhood to senescence: comparison of conventional and new measures based on fractals and chaos theory. Circulation. 1999 Jul 27;100(4):393-9.
[50] Tulppo MP, Hughson RL, Mäkikallio TH, Airaksinen KE, Seppänen T, Huikuri HV. Effects of exercise and passive head-up tilt on fractal and complexity properties of heart rate dynamics. Am J Physiol Heart Circ Physiol. 2001 Mar;280(3):H1081-7.

[51] Reyes del Paso GA, Langewitz W, Mulder LJ, van Roon A, Duschek S. The utility of low frequency heart rate variability as an index of sympathetic cardiac tone: a review with emphasis on a reanalysis of previous studies. Psychophysiology. 2013 May;50(5):477-87.
[52] Tulppo MP, Mäkikallio TH, Takala TE, Seppänen T, Huikuri HV. Quantitative beat-to-beat analysis of heart rate dynamics during exercise. Am J Physiol. 1996 Jul;271(1 Pt 2):H244-52.
[53] Dipla K, Papadopoulos S, Zafeiridis A, Kyparos A, Nikolaidis MG, Vrabas IS. Determinants of muscle metaboreflex and involvement of baroreflex in boys and young men. Eur J Appl Physiol. 2013 Apr;113(4):827-38.
[54] Ichinose M, Saito M, Wada H, Kitano A, Kondo N, Nishiyasu T. Modulation of arterial baroreflex dynamic response during muscle metaboreflex activation in humans. J Physiol. 2002 Nov 1;544(Pt 3):939-48.
[55] Ichinose M, Saito M, Wada H, Kitano A, Kondo N, Nishiyasu T. Modulation of arterial baroreflex control of muscle sympathetic nerve activity by muscle metaboreflex in humans. Am J Physiol Heart Circ Physiol. 2004 Feb;286(2):H701-7.
[56] Ichinose M, Nishiyasu T. Muscle metaboreflex modulates the arterial baroreflex dynamic effects on peripheral vascular conductance in humans. Am J Physiol Heart Circ Physiol. 2005 Apr;288(4):H1532-8.
[57] Cooper VL, Pearson SB, Bowker CM, Elliott MW, Hainsworth R. Interaction of chemoreceptor and baroreceptor reflexes by hypoxia and hypercapnia - a mechanism for promoting hypertension in obstructive sleep apnoea. J Physiol. 2005 Oct 15;568(Pt 2):677-87.
[58] Simmons GH, Manson JM, Halliwill JR. Mild central chemoreflex activation does not alter arterial baroreflex function in healthy humans. J Physiol. 2007 Sep 15;583(Pt 3):1155-63.
[59] Shaffer F, Ginsberg J.P. An overview of heart rate variability metrics and norms. Front. Public Health 2017 Sept 5:258.
[60] Samora M, Teixeira AL, Sabino-Carvalho JL, Vianna LC. Spontaneous cardiac baroreflex sensitivity is enhanced during post-exercise ischemia in men but not in women. Eur J Appl Physiol. 2019 Jan;119(1):103-111.
[61] Van De Borne P, Mezzetti S, Montano N, Narkiewicz K, Degaute JP, Somers VK. Hyperventilation alters arterial baroreflex control of heart rate and muscle sympathetic nerve activity. Am J Physiol Heart Circ Physiol. 2000 Aug;279(2):H536-41.
[62] Castiglioni P, Parati G. Present trends and future directions in the analysis of cardiovascular variability. J Hypertens. 2011 Jul;29(7):1285-8.
[63] Silva LE, Silva CA, Salgado HC, Fazan R Jr. The role of sympathetic and vagal cardiac control on complexity of heart rate dynamics. Am J Physiol Heart Circ Physiol. 2017 Mar 1;312(3):H469-H477.
[64] Copie X, Le Heuzey JY, Iliou MC, Khouri R, Lavergne T, Pousset F, Guize L. Correlation between time-domain measures of heart rate variability and scatterplots in postinfarction patients. Pacing Clin Electrophysiol. 1996 Mar;19(3):342-7.
[65] Contreras P, Canetti R, Migliaro ER. Correlations between frequency-domain HRV indices and lagged Poincaré plot width in healthy and diabetic subjects. Physiol Meas. 2007 Jan;28(1):85-94.
[66] Guzik P, Piskorski J, Krauze T, Schneider R, Wesseling KH, Wykretowicz A, Wysocki H. Correlations between the Poincaré plot and conventional heart rate variability parameters assessed during paced breathing. J Physiol Sci. 2007 Feb;57(1):63-71.

[67] Toichi M, Sugiura T, Murai T, Sengoku A. A new method of assessing cardiac autonomic function and its comparison with spectral analysis and coefficient of variation of R-R interval. J Auton Nerv Syst. 1997 Jan 12;62(1-2):79-84.
[68] Ciccone AB, Siedlik JA, Wecht JM, Deckert JA, Nguyen ND, Weir JP. Reminder: RMSSD and SD1 are identical heart rate variability metrics. Muscle Nerve. 2017 Oct;56(4):674-678.
[69] Bolea J, Pueyo E, Laguna P, Bailón R. Non-linear HRV indices under autonomic nervous system blockade. Conf Proc IEEE Eng Med Biol Soc. 2014;2014:3252-5.
[70] Silva LE, Lataro RM, Castania JA, da Silva CA, Valencia JF, Murta LO Jr, Salgado HC, Fazan R Jr, Porta A. Multiscale entropy analysis of heart rate variability in heart failure, hypertensive, and sinoaortic-denervated rats: classical and refined approaches. Am J Physiol Regul Integr Comp Physiol. 2016 Jul 1;311(1):R150-6.
[71] Bari V, Valencia JF, Vallverdú M, Girardengo G, Marchi A, Bassani T, Caminal P, Cerutti S, George AL Jr, Brink PA, Crotti L, Schwartz PJ, Porta A. Multiscale complexity analysis of the cardiac control identifies asymptomatic and symptomatic patients in long QT syndrome type 1. PLoS One.
[72] Platisa MM, Gal V. Reflection of heart rate regulation on linear and nonlinear heart rate variability measures. Physiol Meas. 2006 Feb;27(2):145-54.
[73] Platisa MM, Gal V. Dependence of heart rate variability on heart period in disease and aging. Physiol Meas. 2006 Oct;27(10):989-98.
[74] Stauss HM. Heart rate variability: just a surrogate for mean heart rate? Hypertension. 2014 Dec;64(6):1184-6.
[75] Monfredi O, Lyashkov AE, Johnsen AB, Inada S, Schneider H, Wang R, Nirmalan M, Wisloff U, Maltsev VA, Lakatta EG, Zhang H, Boyett MR. Biophysical characterization of the underappreciated and important relationship between heart rate variability and heart rate. Hypertension. 2014 Dec;64(6):1334-43.
[76] Sacha J. Interaction between heart rate and heart rate variability. Ann Noninvasive Electrocardiol. 2014 May;19(3):207-16.
[77] Gąsior JS, Sacha J, Jeleń PJ, Pawłowski M, Werner B, Dąbrowski MJ. Interaction Between Heart Rate Variability and Heart Rate in Pediatric Population. Front Physiol. 2015 Dec 18;6:385.
[78] Dias da Silva VJ, Tobaldini E, Rocchetti M, Wu MA, Malfatto G, Montano N, Zaza A. Modulation of sympathetic activity and heart rate variability by ivabradine. Cardiovasc Res. 2015 Oct 1;108(1):31-8.
[80] Yaniv Y, Ahmet I, Liu J, Lyashkov AE, Guiriba TR, Okamoto Y, Ziman BD, Lakatta EG. Synchronization of sinoatrial node pacemaker cell clocks and its autonomic modulation impart complexity to heart beating intervals. Heart Rhythm. 2014 Jul;11(7):1210-9.